Mandala Networks: ultra-robust, ultra-small-world and highly sparse graphs

Cesar I. N. Sampaio Filho[1], André A. Moreira[1], Roberto F. S. Andrade[2], Hans J. Herrmann[1,3], José S. Andrade Jr.[1,3*]
[1] *Departamento de Física, Universidade Federal do Ceará, 60451-970 Fortaleza, Ceará, Brazil*
[2] *Instituto de Física, Universidade Federal da Bahia, 40210-340 Salvador, Bahia, Brazil*
[3] *Computational Physics for Engineering Materials, IfB, ETH Zurich, Schafmattstrasse 6, 8093 Zurich, Switzerland*
(Dated: June 30, 2014)

The increasing demands in security and reliability of infrastructures call for the optimal design of their embedded complex networks topologies. The following question then arises: what is the optimal layout to fulfill best all the demands? Here we present a general solution for this problem with scale-free networks, like the Internet and airline networks. Precisely, we disclose a way to systematically construct networks which are 100% robust against random failures as well as to malicious attacks. Furthermore, as the sizes of these networks increase, their shortest paths become asymptotically invariant and densities of links go to zero, making them ultra-small worlds and highly sparse, respectively. The first property is ideal for communication and navigation purposes, while the second is interesting economically.

PACS numbers: 89.75.Hc, 64.60.aq, 89.20.Hh, 89.75.Da

arXiv:1406.7259v1 [physics.soc-ph] 27 Jun 2014

The tremendous increase in complexity of infrastructural networks, like the Internet and those related with transportation and energy supply, is mandatorily accompanied by requirements of higher standards of system reliability, security and robustness. This trend can only be sustained if these complex networks have the right structure. Under this framework, the scale-free property present in many real networks determines important aspects related with their functionality [1–5]. However, while scale-free networks are usually quite robust against random failures, they typically break down rapidly under malicious attacks [6–11]. Numerical studies have recently revealed that this weakness can be mitigated if their structure becomes onion-like, which means that nodes of equal degree are connected among each other and to nodes of higher degree [12, 13]. Since then, the properties of onion-like structures have been extensively investigated [14–23]. Based on this insight, here we will address the challenge of providing a paradigm for complex networks with better topology. More precisely, we show that it is possible to design a family of scale-free networks which are completely robust to random failures as well as to malicious attacks. Additionally, these networks also exhibit other improved properties, like a finite shortest path and extreme sparseness in the thermodynamic limit, which substantially increases communication and reduces costs. Thus these new networks become potential candidates for the design and implementation of complex infrastructural networks.

In the deterministic network model introduced here, the nodes belonging to a given shell have intra-shell and inter-shell connections, and the most connected nodes (hubs) are localized in the innermost shells. The network is recurrently expanded in such a way that every new generation corresponds to the addition of a new shell. Examples of these networks with four shells are shown in Figs. 1(a) and (b). Here we coin the name *mandala network* for this new family of graphs. In the first case, thereafter called network A, the first generation consists of a nucleus with three central nodes forming a complete graph (first shell). From each node in this nucleus, two new nodes emerge to form a connected ring of six nodes, composing the second shell of the second generation network. Following this iterative process, the third shell in the third generation network has an additional connected ring with twelve nodes, which, at this point, must also be linked to their respective ancestral nodes in the first and second shells. The same rules then apply for all new shells present in higher generation networks. This design therefore imposes that nodes at the same shell have the same degree. More precisely, the degree k_{ig} of a node at the i-*th* shell in the g-*th* network generation is given by,

$$k_{ig} = 2^{g-i+1} + (i-1). \tag{1}$$

Defining n_i as the number of nodes in the i-*th* shell, by construction, we have that $n_{i+1} = 2n_i$. From this relation, the number of nodes in the network is given by $N = \sum_{i=1}^{g} n_i$, where the summation is over the total number g of shells.

In fact, the network described so far in Fig. 1(a) is a particular case resulting from the recursive method proposed here to generate an ensemble of ultra-robust networks. For example, in Fig. 1(b) we show another example of mandala network, thereafter named network B. Precisely, the method depends on a set of three parameters, (n_1, b, λ), namely,

* Correspondence to: soares@fisica.ufc.br

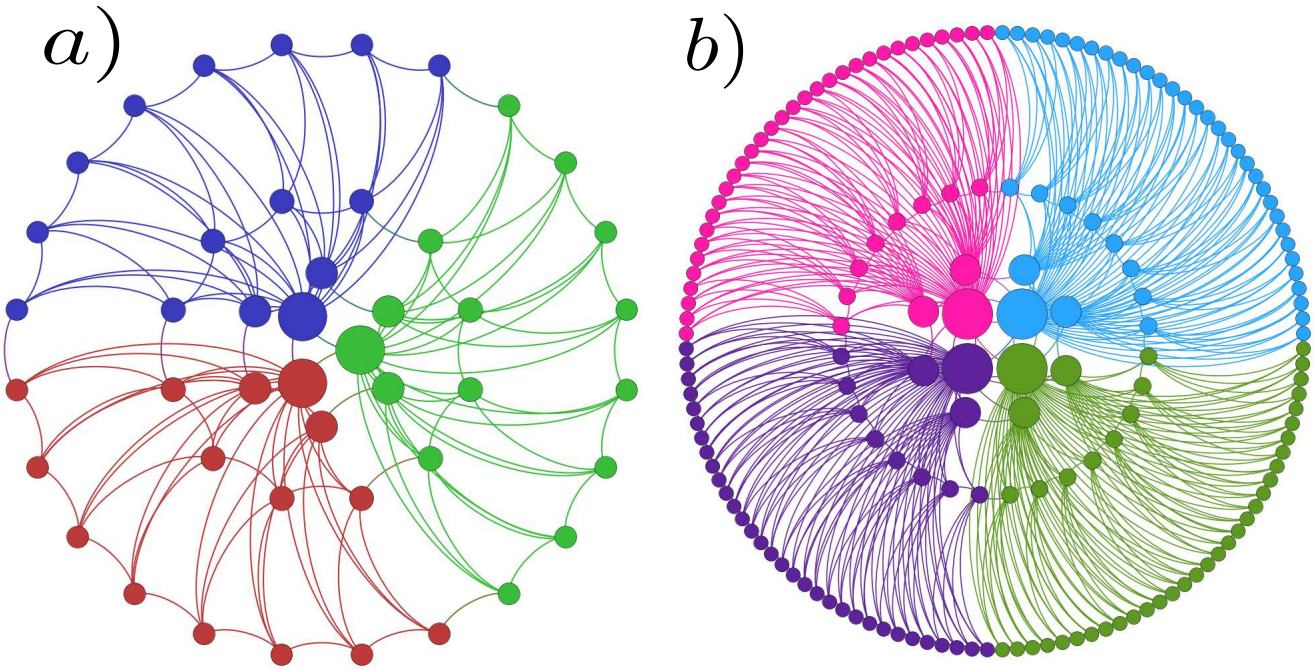

FIG. 1: (Color online) (a) Representation of the mandala network of type A, generated with parameters $b = 2$, $n_1 = 3$ and $\lambda = 2$. The nodes correspond to circles whose areas are proportional to degree, and nodes in the same community have the same color. The first generation consists of a complete graph with three nodes defining the nucleus of the network. To each one of these nodes, two new nodes are connected to form a connected circular ring of six nodes, corresponding to the second shell. Next, the most external nodes generate two new nodes forming a circular ring with twelve nodes (third shell). Every node in the same community is connected with all its ancestral ones. (b) Network of type B, generated with parameters $b = 4$, $n_1 = 4$ and $\lambda = 2$.

the number of nodes in the first generation, n_1, the number of new nodes added to each node in the more external shell, b, and the scale factor, λ, for node degree in successive generations. For instance, the networks A and B are completely defined by the sets $(3, 2, 2)$ and $(4, 4, 2)$, respectively.

Results

Scale-free networks. Any network generated by this method has discrete degree spectra. In order to characterize the scale-free dependence, we consider the cumulative degree distribution, $P(k) = \sum_{k' \geq k} n(k')/N$. Taking into account that in each shell all nodes have the same degree, the cumulative distribution can be written as, $P(k_{ig}) = \sum_{j=1}^{i} n_j/N$. Applying Eq. (1) and the relation $n_{j+1} = bn_j$, it can be shown that the cumulative distribution decays in the form, $P(k_{ig}) \sim 1/k_{ig}$. In Fig. 2, we show a logarithmic plot of the cumulative degree distribution for networks A and B. In both cases, we have the same scale-free dependence. At this point, an explanation about the exponent of the degree distribution becomes necessary [24–26]. By definition of our network, the discrete degree distribution, $p(k)$, can be described by, $p(k_{ig}) \equiv n_i/N$, for a large number of shells. Considering that $n_i \sim 2^i$, we have $p(k_{ig}) \sim 1/k_{ig}$. Therefore, the cumulative and probability distributions scale in the same form. However, if we choose to work with binned intervals between consecutive degrees, the degree distribution is calculated as, $\overline{p}(k_{ig}) \equiv n_i/N\Delta k_{ig}$, where $\Delta k_{ig} = k_{ig} - k_{(i+1)g}$ is the width of the interval. As $\Delta k_{ig} \sim k_{ig}$, it is possible to show that then $\overline{p}(k_{ig}) \sim 1/k_{ig}^2$.

Ultra-small-world networks. Another important property of the mandala networks relates to the mean shortest path length $\langle \ell \rangle = \sum_{ij}^{N} \ell_{ij} / [N(N-1)]$, where ℓ_{ij} is the shortest distance between any two nodes i and j in the network, and the summation goes over all possible node pairs in the system. In our case, this expression can be written in a more convenient form as,

$$\langle \ell \rangle = \frac{1}{N(N-1)} \sum_{j=1}^{g} n_j \phi_j, \tag{2}$$

where $\phi_j = \sum_{k=1}^{N} \ell_{jk}$ is the sum of the shortest path lengths connecting a node in the j-th shell with all other nodes in the network, n_j is the number of nodes in the j-th shell, and the summation goes over the number of shells. Using the

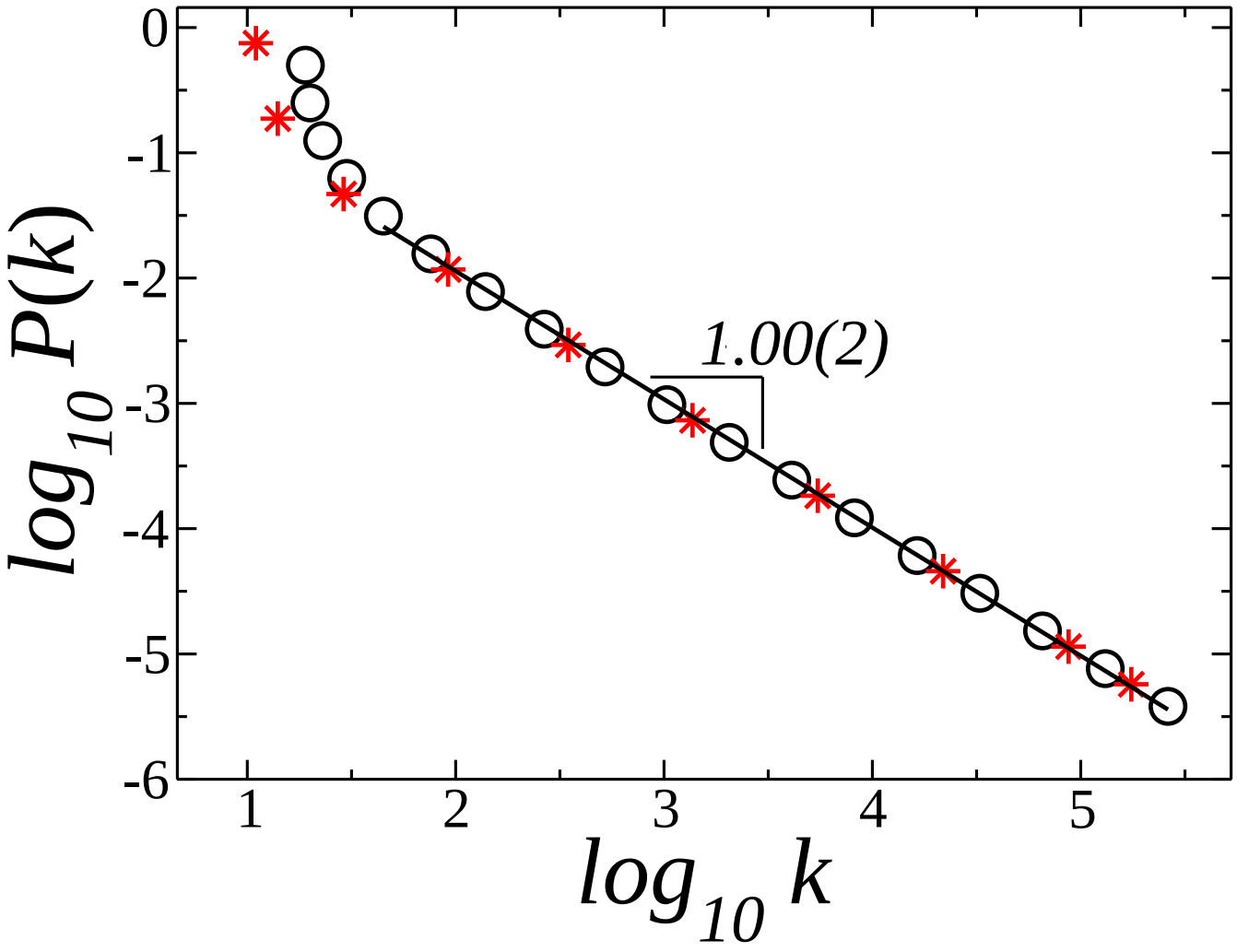

FIG. 2: (Color online) Logarithmic plot of the cumulative degree distribution for the networks A (black circles) and B (red stars). The solid line represents the least-squares fit to data in the scaling regions of a power law, $P(k) \sim k^{-\beta}$, with $\beta = 1.00 \pm 0.02$, which confirms our analytical result.

symmetry of the network A, for example, it is possible to show that $\phi_j = \alpha_j N + \xi_j$, where ξ_j has different values for different shells, and α_i is given by 5/3, 7/3, 5/2, 31/12, 63/24, for $i = 1, 2, 3, 4$, and 5, respectively, so that $\alpha \to 8/3$, for $i \to \infty$. Taking into account the linear dependence of ϕ_j with N and considering the relations for n_j, Eq. (2) reduces to

$$\langle \ell \rangle = \alpha + \frac{O(N)}{N^2}, \tag{3}$$

which leads to $\langle \ell \rangle \to 8/3$ in the thermodynamic limit, $N \to \infty$. We show in Fig. 3 a semi-log plot of the mean shortest path length as a function of the number of nodes. The asymptotic convergence confirms our analytical result and therefore indicates that our network has an ultra-small-world behavior, namely $\langle \ell \rangle$ becomes independent of N. One should note, however, that this result is still different from the case of a complete graph, for which $\langle \ell \rangle = 1$, corresponding to the mean-field limit. Applying a similar sequence of calculations to the network B, it can be readily shown that the mean shortest path length for this topology also converges to a constant in the limit of large system sizes, but now equal to 11/4.

Highly sparse graphs. Next, we define the density d of connections as the ratio between the number of existing connections and the maximal number of possible connections for an undirected network with N nodes, $d = \sum_i n_i k_{ig} / [N(N-1)]$. Considering the expression for k_{ig} given by Eq. (1), we can rewrite the definition of d in

the following way:

$$d = \frac{1}{N(N-1)} \left[\sum_{i}^{g} n_i 2^{g-i+1} + \sum_{i}^{g} n_i (i-1) \right]. \tag{4}$$

Expressing both summations in Eq. (4) in terms of the number of nodes in the network, $N = \sum_i^g n_i$, and considering the limit of a very large number of generations, we obtain,

$$d \sim \frac{1}{N} \log N^2. \tag{5}$$

The inset of Fig. 3 shows the dependence of the density of connections on the number of nodes for networks of type A, confirming the asymptotic behavior predicted by Eq. (5). In the case of network B, where the number of new nodes generated is twice that of network A, the density of connections decays faster. Indeed, applying the same approach and considering $b = 4$, it is possible to show for network B that $d \sim (\log N)/N$. As a consequence, we conclude that our networks, despite of their ultra-small-world property, are extremely sparse when compared to the behavior of a complete graph, $d = 1$, and has only logarithmic correction to $d \sim 1/N$ that is valid for the Erdös-Rényi network at the percolation threshold.

Ultra-robust graphs. The framework of percolation is usually considered for the analysis of the robustness of complex networks [7, 22, 27–33]. In this context, robustness is typically quantified by the critical fraction q_c of removed nodes that leads to a total collapse of the network [6, 9, 10, 12]. Nevertheless, as previously reported [12–14, 16], this approach does not account for situations in which the system can suffer a big damage without breaking down completely. The size of the giant component during the removal process of nodes has been recently introduced [12] as a new measure to robustness,

$$R = \frac{1}{N+1} \sum_{Q=1}^{N} s, \tag{6}$$

where s is the fraction of nodes belonging to the giant component after removing $Q = qN$ nodes, q is the fraction of nodes removed, and R is in the range $[0, 1/2]$. The limit $R = 0$ corresponds to a system of isolated nodes, while $R = 1/2$ to the most robust network, which is the case, for example, of a completely connected graph. Here we check the robustness of our complex network model when subjected to both mechanisms of malicious and random attacks [6–10].

Considering that the targets of malicious attacks are the surviving nodes with highest degree, in our network model, the process starts by selecting one of the nodes of the first shell. The deletion of such node will not cause the removal of other nodes, since any node in any shell has links to nodes in the previous and subsequent shells. Thus, the number of nodes of the giant component decreases only by one. The same occurs until all nodes in the first shell are erased. The attacks are then directed to the nodes in the second shell, but again all nodes in the second shell are connected to nodes in the next shells, so that the same argument applies. Thus, it follows that, $s = 1 - q$, which is valid up to the point when the remaining nodes are located in the last shell. This behavior is confirmed by results of numerical simulations shown in the main plot of Fig. 4 (dashed line), regardless of the size and the type A or B of the network. It shows further that the integrity of the giant component is maintained up to nearly its total breakdown for either malicious or random strategies of node removal. Interestingly, the results in Fig. 4 also indicate that random attacks are generally more efficient than malicious ones.

From the behavior of s and Eq. (6), the robustness R to malicious attacks can be calculated as, $R = \sum_i^{N-1}(N - i)/(N+1) = (2N+1)/2N$. As shown in the inset of Fig. 4, R converges asymptotically towards the maximum value, $R_{max} = 1/2$, as expected for the case of malicious attacks to sufficiently large networks A and B. Mandala networks of different types and sizes also behave similarly when subjected to random attacks. Nevertheless, even for random failures, the level of robustness for our networks is superior when compared to other networks [12], with $R \approx 0.45$ for type A, and $R \approx 0.43$, for type B.

The Ising model. In small-world networks, the fact that the diameter of the graph does not grow faster than $\log N$ implies an infinite dimension. Mean-field theories therefore can successfully describe their critical behavior [1, 34–38]. In order to investigate how collective ordering emerges in mandala networks, for which the shortest-path length is independent on N, we consider Ising spins σ_i associated to their nodes and ferromagnetic interactions J between them on the edges. Adopting the reduced Hamiltonian, $\mathcal{H}/k_bT = -J \sum_{ij} \sigma_i \sigma_j$, we perform Monte Carlo (MC) simulations on networks of type A for different system sizes N and temperature T values. In particular, we analyse the finite-size scaling properties of the model at the critical temperature. The results in Fig. 5 show that the

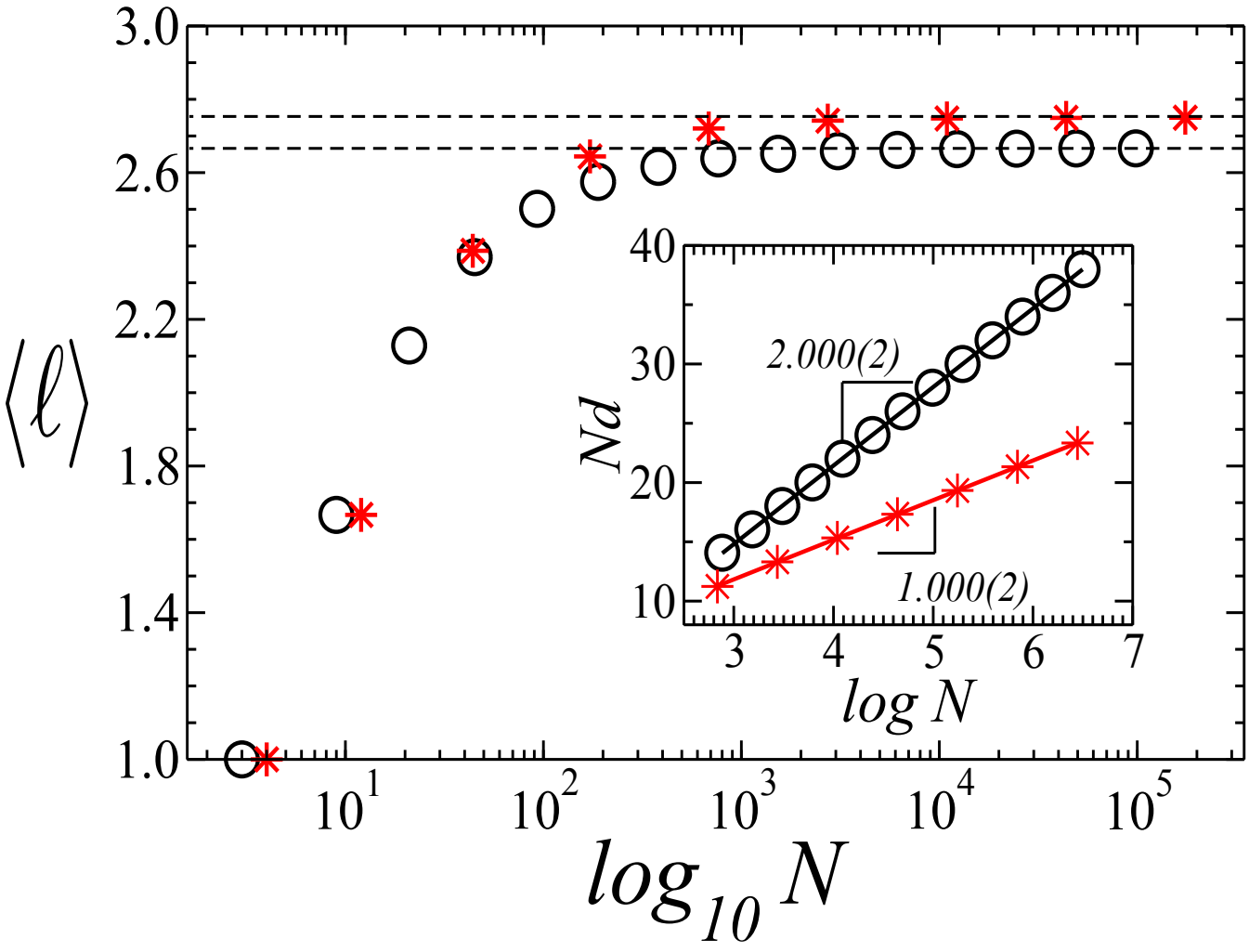

FIG. 3: (Color online) Semi-log plot showing the dependence of the mean shortest path length $\langle \ell \rangle$ on the number of nodes N, for the networks A (black circles) and B (red stars). As depicted, the mean shortest-path lengths of A and B converge to the values 8/3 (top dashed line) and 11/4 (bottom dashed line), respectively, in the limit of a large number of nodes. Therefore, both networks can be considered as ultra-small worlds. The inset shows the semi-log plot of the density of connections d as a function of the number of nodes N in log-linear scale. Our analytical results reveal that $d \sim \frac{1}{N} \log N^2$ (black circles) for network A, while network B behaves as $d \sim \frac{1}{N} \log N$ (red stars). The solid lines are the best fits to the numerically generated data sets, confirming these predicted behaviors. Hence both networks are highly sparse.

divergence of the finite-size critical temperature with N, measured from the peak of the susceptibility, has the form, $T_c(N) \sim N^{1/\overline{\nu}}$, with a critical exponent, $1/\overline{\nu} = 0.50 \pm 0.01$.

Discussion

In summary, we have presented a recursive method to generate an ensemble of ultra-robust networks defined by a set of three parameters, namely (n_1, b, λ). We have shown that the networks originated from our model have scale-free topologies and are ultra-robust either against malicious attacks or random failures of nodes. From analytical calculations confirmed through numerical simulation results, we have demonstrated that these networks are also ultra-small, i.e., the average shortest-path lengths of sufficiently large networks become independent of their number of nodes. Surprisingly, our results also show that, as compared to a complete graph, which is also ultra-small and ultra-robust, these networks are highly sparse, with the density of edges going to zero with system size. Finally, we have verified that the critical temperature of the Ising model on the mandala network topology diverges with system size according to a power-law dependence, described by an exponent $1/\overline{\nu} = 0.50 \pm 0.01$. We expect to generalize this last result to other universality classes, for example, considering directed percolation and self-organized models on our deterministic networks.

Methods

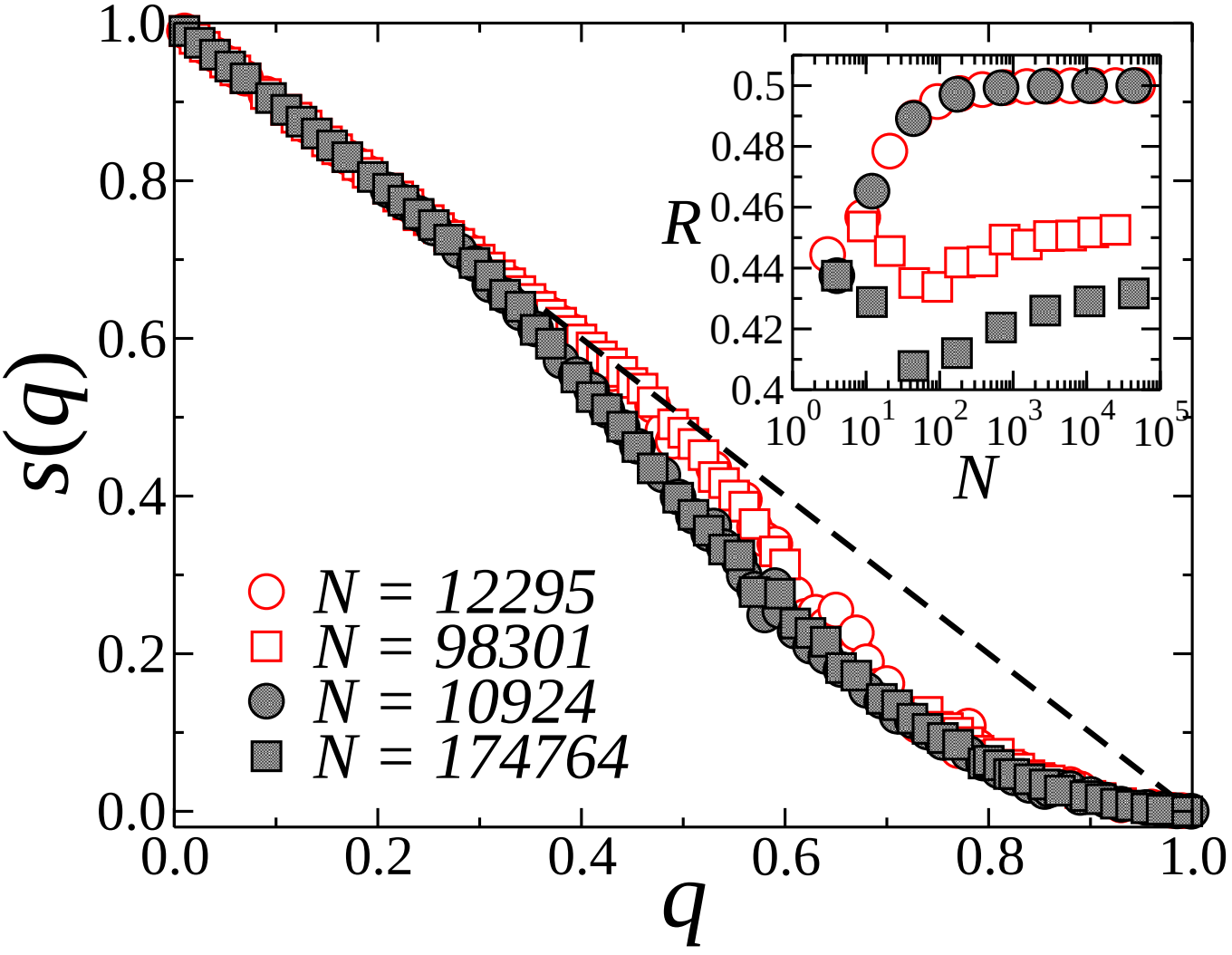

FIG. 4: (Color online) Fraction $s(q)$ of nodes belonging to the spanning cluster as a function of the fraction of removed nodes q, for malicious attacks targeted by degree (dashed line) and random removals (symbols) of nodes. In the case of malicious attacks, an identical behavior is observed for sufficiently large networks, $s = 1-q$, regardless of the type (A or B) of the network used in the calculations. In the random-attack case, our results exhibit high robustness for both A and B networks, that are also shown to be practically independent of the network size for the different numbers of nodes N considered. The inset shows the robustness measure R as a function of N for networks A and B subjected to malicious attacks targeted by degree (open symbols) as well as random failures (closed symbols). An asymptotic convergence towards the maximum robustness value, $R_{max} = 1/2$, is observed for the case of malicious attacks, regardless of the network type. Both networks are less resilient to random attacks than to targeted ones, but still rather robust as compared to other models and real networks [12], with $R \approx 0.45$ and 0.43, for types A and B, respectively.

The Ising model. The Monte Carlo simulations of the Ising model on the mandala networks were performed using the Metropolis algorithm, starting from different initial spin configurations. In order to study the critical behavior of the system, we considered the magnetization M_L and the susceptibility χ_L, which are defined by

$$M_N(T) = \langle \langle m \rangle_{time} \rangle_{sample} \,, \tag{7}$$

$$\chi_N(T) = N \left[\left\langle \langle m^2 \rangle_{time} - \langle m \rangle^2_{time} \right\rangle_{sample} \right], \tag{8}$$

where $\langle m \rangle = |\frac{1}{N} \sum_{i=1}^{N} \sigma_i|$, T is the temperature and N is the total number of nodes in network. The symbols $< \cdots >_{time}$ and $< \cdots >_{sample}$, respectively, denote time averages taken in the stationary state and configurational

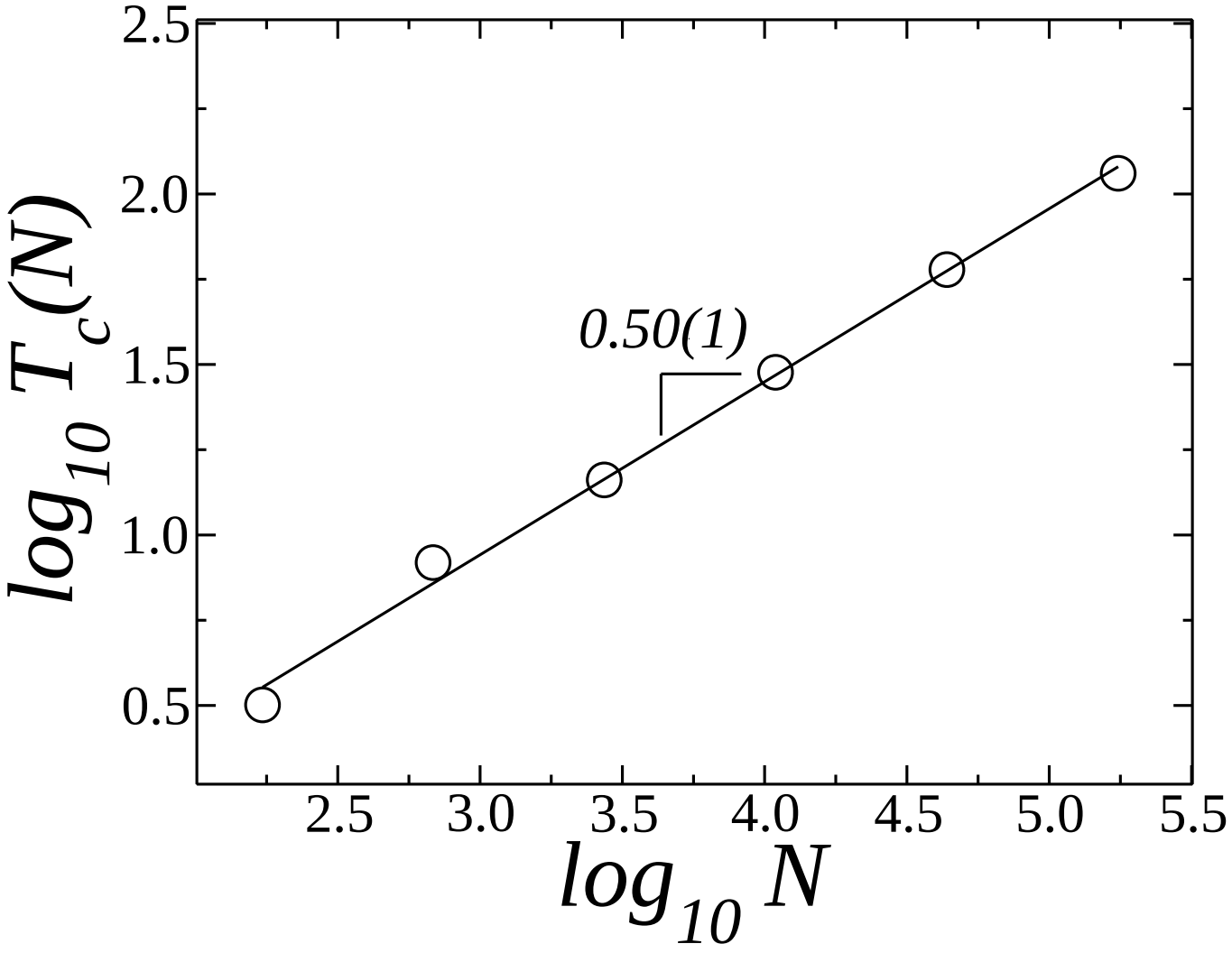

FIG. 5: Log-log plot showing the finite-size scaling analysis for the critical temperature of the Ising model implemented on the network model A. The critical temperature diverges according to a power-law dependence, $T_c(N) \sim N^{1/\overline{\nu}}$, with $1/\overline{\nu} = 0.50 \pm 0.01$.

averages taken over 100 independent samples. Time is measured in Monte Carlo steps (MCS), and 1 MCS corresponds to N attempts of changing the states of the spins. In our simulations, the initial 10^5 MCS were utilized to guarantee the system reached the steady state, after which the time averages were estimated using the next 6×10^5 MCS.The value of temperature where χ_N has a maximum is identified as $T_c(N)$ for $N = 172, 684, 2732, 10924, 43692,$ and 174764.

[1] Albert, R. and Barabási, A.-L. Statistical mechanics of complex networks. *Rev. Mod. Phys.* **74**, 031109 (2002).
[2] Newman, M. The structure and function of complex networks. *SIAM Review* **45**, 167 (2003).
[3] López, E. and Buldyrev, S.V. and Havlin, S. and Stanley, H.E. Anomalous transport in scale-free networks. *Phys. Rev. Lett.* **94**, 248701 (2005).
[4] Boccaletti, S. and Latora, V. and Moreno, Y. and Chavez, M. and Hwang, D. -U. Complex networks: Structure and dynamics. *Phys. Rep.* **424**, 175 (2006).
[5] Barabási, A.-L. Scale-free networks: A decade and beyond . *Science* **325**, 412 (2009).
[6] Albert. R., Jeong H, and Barabási A.-L., Error and attack tolerance of complex networks, *Nature* **406**, 378 (2000).
[7] Callaway D. S., Newman M. E. J., Strogatz S. H., and Watts D. J., Network Robustness and Fragility: Percolation on Random Graphs, *Phys. Rev. Lett.* **85**, 5468 (2000).
[8] Cohen R., Erez K., ben Avraham D., and Havlin S., Resilience of the Internet to Random Breakdowns, *Phys. Rev. Lett.*

85, 4626 (2000).
[9] Cohen R., Erez K., ben Avraham D., and Havlin S., Breakdown of the Internet under Intentional Attack, *Phys. Rev. Lett.* **86**, 3682 (2001).
[10] Holme P., Holme B. J., Yoon C. N., and Han S. K., Attack vulnerability of complex networks, *Phys. Rev. E* **65**, 056109 (2002).
[11] Tanizawa T., Paul G., Cohen R., Havlin S., and Stanley H. E., Optimization of network robustness to waves of targeted and random attacks, *Phys. Rev. E* **71**, 047101 (2005).
[12] Schneider C. M., Moreira A. A., Andrade J. S., Havlin S., and Herrmann H. J., Mitigation of malicious attacks on networks, *Proc. Natl. Acad. Sci.* **108**, 3838 (2011).
[13] Herrmann H. J., Schneider C. H., Moreira A. A., Andrade J. S., and Havlin S., Onion-like network topology enhances robustness against malicious attacks, *J. Stat. Mech.: Theory Exp.* **01**, 01027 (2011).
[14] Wu Z.-X. and Holme P., Onion structure and network robustness, *Phys. Rev. E* **84**, 026106 (2011).
[15] Valdez L. D., Buono C., Braunstein L. A., and Macri P. A., Effect of degree correlations above the first shell on the percolation transition, *Europhys. Lett.* **96**, 38001 (2011).
[16] Schneider C. H., Mihaljev T., and Herrmann H. J., Inverse targeting An effective immunization strategy, *Europhys. Lett.* **98**, 46002 (2012).
[17] Tanizawa T., Havlin S., and Stanley H. E., Robustness of Onionlike Correlated Networks against Targeted Attacks, *Phys. Rev. E* **85**, 046109 (2012).
[18] Zeng A. and Liu W, Enhancing network robustness against malicious attacks, *Phys. Rev. E* **85**, 066130 (2012).
[19] Helbing D., Globally networked risks and how to respond, *Nature* **497**, 51 (2013).
[20] Dong G. et al., Robustness of network of networks under targeted attack, *Phys. Rev. E* **87**, 052804 (2013).
[21] Skarpalezos L., Kittas A., Argyrakis P., Cohen R., and Havlin S., Anomalous biased diffusion in networks, *Phys. Rev. E* **88**, 012817 (2013).
[22] Wang B., Gao L., Gao Y., and Deng Y., Maintain the structural controllability under malicious attacks on directed networks, *Europhys. Lett.* **101**, 58003 (2013).
[23] Louzada V. H. P., Daolio F., Herrmann H. J., and Tomassini M., Smart rewiring for network robustness, *J. Complex Netw.* **1**, 150 (2013).
[24] Andrade J. S., Herrmann H. J., Andrade R. F. S., and da Silva L. R., Apollonian Networks: Simultaneously Scale-Free, Small World, Euclidean, Space Filling, and with Matching Graphs, *Phys. Rev. Lett.* **102**, 079901 (2009).
[25] Guo J.-L. and Wang L.-N., *Physics Procedia* **3**, 1791 (2010).
[26] Mungan M., Comment on Apollonian Networks: Simultaneously Scale-Free, Small World, Euclidean, Space Filling, and with Matching, *Phys. Rev. Lett.* **106**, 029802 (2011).
[27] Newman M. E. J. and R. M. Ziff, Fast Monte Carlo algorithm for site or bond percolation, *Phys. Rev. E* **64**, 016706 (2001).
[28] Cohen R., Havlin S., and ben Avraham D., Efficient Immunization Strategies for Computer Networks and Populations, *Phys. Rev. Lett.* **91**, 247901 (2003).
[29] Moreira A. A., Andrade J. S., Herrmann H. J., and Indekeu J. O., How to Make a Fragile Network Robust and Vice Versa, *Phys. Rev. Lett.* **102**, 018701 (2009).
[30] Hooyberghs H. et al., Biased percolation on scale-free networks, *Phys. Rev. E* **81**, 011102 (2010).
[31] Newman M. E. J., Communities, modules and large-scale structure in networks, *Nature Phys.* **8**, 25 (2011).
[32] Peixoto T. P. and Bornholdt S., Evolution of Robust Network Topologies: Emergence of Central Backbones, *Phys. Rev. Lett.* **109**, 118703 (2012).
[33] Taylor D. and Restrepo J. G., A network-specific approach to percolation in complex networks with bidirectional links, *Europhys. Lett.* **98**, 16007 (2012).
[34] Newman M E. J. and Watts D. J., Scaling and percolation in the small-world network model, *Phys. Rev. E* **60**, 7332 (1999).
[35] Giuraniuc C. V. et al., Trading Interactions for Topology in Scale-Free Networks, *Phys. Rev. Lett.* **95**, 098701 (2005).
[36] Dorogovtsev S. N., Goltsev A. V., and Mendes J. F. F., Critical phenomena in complex networks, *Rev. Mod. Phys.* **80**, 1275 (2008).
[37] Castellano C. and Pastor-Satorras R., Routes to Thermodynamic Limit on Scale-Free Networks, *Phys. Rev. Lett.* **100**, 148701 (2008).
[38] Ferreira S. C., Ferreira R. S., Castellano C., and Pastor-Satorras R., Quasi-stationary simulations of the contact process on quenched networks, *Phys. Rev. E* **84**, 066102 (2011).

Acknowledgments

We thank the Brazilian agencies CNPq, CAPES, FUNCAP, and FAPESB, the National Institute of Science and Technology for Complex Systems (INCT-SC Brazil), to the ETH Risk Center (Switzerland), and the European Research Council through Grant FlowCSS No. FP7-319968 for financial support.

Authors contributions

The authors C.S.F., A.M., R.A., H.J.H., and J.S.J., contributed equally.

Additional information

Competing financial interests: The authors declare no competing financial interests.